ANALYSIS OF THE ADVANTAGES AND LIMITATIONS OF STATIONARY IMAGING FOURIER TRANSFORM SPECTROMETER*

BRIAN P. BEECKEN† and RANDALL R. KLEINMAN‡
Physics Department, Bethel University, St. Paul, MN 55112

March 14, 2003
rev. July 14, 2004

New developments in infrared sensor technology have potentially made possible a new space-based system which can measure far-infrared radiation at lower costs (mass, power and expense). The Stationary Imaging Fourier Transform Spectrometer (SIFTS), proposed by NASA Langley Research Center, makes use of new detector array technology. A mathematical model which simulates resolution and spectral range relationships has been developed for analyzing the utility of such a radically new approach to spectroscopy. Calculations with this forward model emulate the effects of a detector array on the ability to retrieve accurate spectral features. Initial computations indicate significant attenuation at high wavenumbers.

1 Introduction

Passive remote sensors being used for atmospheric observation are often Michelson interferometers, which usually are larger instruments that gather interferometric data utilizing a moving mirror. The use of laser metrology for determining exact mirror displacements and the power consumption of extra components such as motors and telemetry to report mirror positions make them a costly intstrument.[1]

The SIFTS system (Stationary Infrared Fourier Transform Spectrometer), as proposed by the NASA Langley Research Center, would use the stationary interferometry of a Common-path (also known as a Sagnac) interferometer and take distinct advantage of continuing advances in infrared detector arrays. Since it would require no moving parts, the mass and power limitations of space-based sensors will be more easily realized.

Virtual source configurations have the advantage of a minimum of optical components and fixed placement of those components. Of the virtual source configurations, the Common-Path interferometer was chosen because of its high yield of incident energy captured on a detector array. Furthermore, as the name implies, the two beams that it produces follow a common path. Therefore, any disturbance in one arm of the interferometer will affect both beams and no resultant changes will occur in the interference pattern. The result is an instrument that is inherently insensitive to vibrations.

Because of the absence of definitive experimental data in the far infrared region of the earth's

*Research funded by Bethel University and NASA Research Grant #: NAG-1-02012

†beebri@bethel.edu; phone 651-638-6334

‡Currently with the Department of Theoretical and Applied Mechanics, University of Illinois, Champaign-Urbana.

emission spectrum, the intended range of SIFTS is 10–1000 μm. Examination of this region is of great importance because up to half of the outgoing radiation of the earth occurs at these wavenumbers. Water vapor is known to radiate in this region, creating a large data gap in stratospheric chemistry, climate forecasting and tropospheric cooling by radiative emission. Also, cirrus clouds are known to block far-IR radiation, but the degree is not known due to lack of observational data.[1]

Many commercial applications also exist such as industrial process control in paper production and environmental monitoring of smokestack gas emissions. SIFTS would enhance the ability to do qualitative and quantitative chemical measurements.[1]

Whereas both the SIFTS system and a Michelson will create an optical path length difference (OPD) and resulting fringe pattern, the process by which this interference pattern is created and represented digitally will be different despite the pattern being the same. Since the Michelson will be scanned incrementally, the fringes of the interference effectively collapse to a point and thus only a single detector element is required.

However, the SIFTS system will display the whole interference pattern on a multi-element detector array allowing for faster data acquisition, but different issues relating to resolution. The resolution of SIFTS will be limited by the number, size, and placement of the detector elements. Unlike the Michelson, simply increasing the path length difference to get higher resolution is not easily done. Therefore, analysis of the effects of the detector array on the ability to reproduce true spectral features will be essential in the development of the sensor and its evaluation.

Previous investigations done with multi-element detector arrays by NASA indicate that wavenumber resolutions of 1–2 cm^{-1} should be attainable with 500 to 1,000 detector elements in an array.[1] The spectral resolution of SIFTS will ultimately depend on the number of elements in the array used and will be limited by the Nyquist Criterion.

The goal of the present research is to develop a computational model that takes a particular spectrogram and computes the inteferogram that the Common Path interferometer produces. The model can then use the characteristics of a hypothetical detector array (e.g., number of detectors, fill factor, nonuniformity) to calculate what the retrieved spectrum will look like. The model will allow us to determine how various detector characteristics effect the resolution of the instrument.

2 The Computational Model

2.1 Notation

The SIFTS system will differ from a Michelson in both the way that the interferogram is created and the way it is converted to a discrete set of digital data via the detector array. The interference pattern created by SIFTS will be projected onto the detector array. Because a detector averages across its active area, the width of each pixel is analogous to the limitation due to the size of the mirror movement increments in the Michelson. It is assumed that the interferogram will have a scalable width so the entire array will receive radiation. Then for SIFTS the ratio of the width of each pixel to the size of the interferogram is analogous to the ratio of the size of a mirror increment to the total distance the mirror travels in the Michelson.

Because of these differences, relationships need to be specified for the SIFTS system. A mathematical relation exists between the maximum and minimum OPDs (x_{max} and x_{min}), the maximum and minimum unaliased wavenumbers (σ_{max} and σ_{min}), and the respective resolutions of the interferogram and spectrogram, Δx and $\Delta\sigma$. Note that $\sigma \equiv \lambda^{-1}(\text{cm}^{-1}) = \frac{\nu}{c}$ with c in cm/sec. Variables representing parameters after the radiation has been detected by the array will be denoted with a prime. For example, $\Delta\sigma'$ is the spectral resolution of the retrieved spectrum and $\Delta x'$ is the effective detector width.

Real spectral emmissions are continuous, but any data for used as input spectrograms will be discrete. Therefore, the model will produce an artificially discrete interferogram rather than the continuous interferogram that the actual SIFTS system will produce. The model calculates how

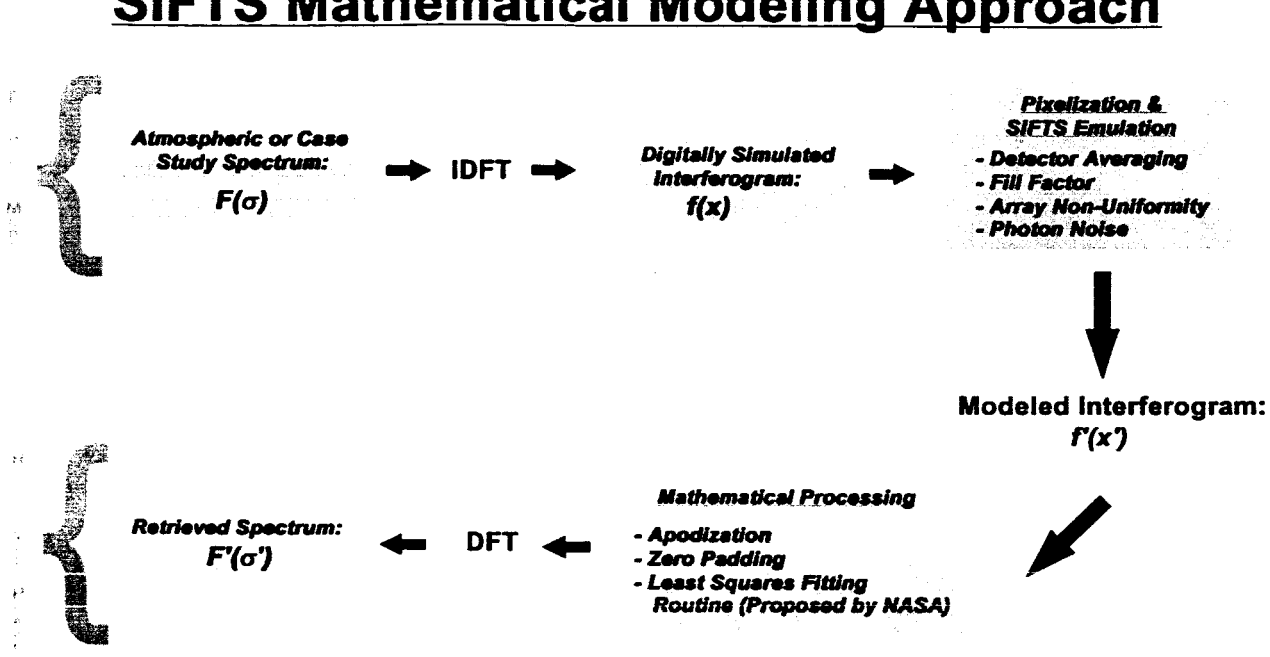

Figure 1: Schematic diagram of the SIFTS Modeling Approach.

the discrete inteferogram is imaged by the discrete detector array. We will use N to denote the number of points in an original atmospheric spectrum and N' for the number of detectors. In order to better simulate reality, we will need to make sure that N is sufficiently larger than N'. The number of detectors N will also determine the maximum number of points that can be used in the calculation of the retrieved spectrum.

Figure 1 illustrates in schematic form the important features of the computational model. The model is written in MATLAB[1] because of its ease of handling discrete data and exceptional graphing capabilities.

2.2 The Forward Model

The computational model is comprised of two separate phases: the forward model and the retrieval phase. The forward model takes data from an atmospheric spectrum that may consist of data derived from previous experiment or, for testing purposes, a fabricated spectrum. This initial spectrogram is called $F(\sigma)$. Then, the forward model uses an Inverse Discrete Fourier Transform (IDFT) to convert the spectrum into the digitally simulated interference pattern called $f(x)$. See Fig. 1.

Once the simulated interference pattern is generated, four parameters are needed to realistically simulate the detector array. These parameters are necessary because of the effects caused by the pixelization of the interferogram. They include:

1. averaging the incident radiation across the pixel's active area
2. the percentage of the detector element width that is actually sensitive, called the "fill factor"
3. non-uniformity of the detector elements
4. the background and/or photon noise encountered by all detectors.

[1]The MathWorks, Inc., 3 Apple Hill Drive, Natick, MA 01760; www.mathworks.com.

The output of the forward model is a simulated interferogram $f'(x')$ that accounts for the effects of pixelization by the detector array. Thus, the effects on the inteferogram of various detector characteristics can be studied. The symbol $\Delta x'$ represents the pixel spacing, $x'_{\max}$ represents the total length of the array, and N' is the total number of detector elements.

In summary, the order of the forward model is:

$$F(\sigma) \rightarrow \text{IDFT} \rightarrow f(x) \rightarrow \text{Pixelization} \rightarrow f'(x')$$

2.3 The Retrieval Phase

Once the inteferogram as "seen" by the detector array is simulated, the retrieval phase of the computational model converts $f'(x')$ into a spectrogram using a Discrete Fourier Transform (DFT). This retrieved spectrum $F'(\sigma')$ can then be compared to the original spectrum $F(\sigma)$ in order to determine the accuracy with which SIFTS measures the spectrum. Standard mathematical processing techniques are used in this phase. These processes will be discussed in Section 3.

The order of the retrieval phase is:

$$f'(x') \rightarrow \text{Processing} \rightarrow \text{DFT} \rightarrow F'(\sigma')$$

3 Mathematical Review

3.1 The Discrete Fourier Transform

Equation (1) shows how a computer calculates the discrete Fourier transform of $f(x)$.

$$F(\sigma) = N^{-1} \sum_{j=1}^{N} f(x) e^{-2\pi i (\frac{\sigma}{N}) x_j} \qquad (1)$$

For spectroscopy, $F(\sigma)$ signifies the spectrogram, (i.e., the discrete representation of the spectral features), and the interferogram is $f(x)$. A commonly used shorthand notation for Eq. (1) is

$$f(x) \supset F(\sigma) \qquad (2)$$

which means that the discrete Fourier transform of $f(x)$ is $F(\sigma)$. Equation (3) is used for calculating the inverse discrete Fourier transform, which also happens to be the Fourier transform of $F(\sigma)$.[4]

$$f(x) = \sum_{j=1}^{N} F(\sigma) e^{2\pi i (\frac{x}{N}) \sigma_j} \qquad (3)$$

In these equations, N denotes the number of data points in the spectrogram or interferogram. When considering pixelized data sets created by the forward model, the appropriate prime notation would need to be used in Eqs. (1, 3).

3.2 Convolution

Convolution is a very unique and useful tool within the mathematics of Fourier transforms. It simply states that the Fourier transform of a product of two functions will be the product of the separate functions' Fourier transforms.[2] Often the symbol $\star$ is used to represent the convolution operator:

$$f_1(x) \star f_2(x) \supset F_1(\sigma) F_2(\sigma) \qquad (4)$$

The convolution operation is a valuable tool because it allows a function to be modified so that the outcome in the transformed domain is improved.

3.3 Apodization

Literally speaking, apodization means *foot removal.*[3] When considering Fourier spectroscopy, the experimentally determined OPDs will always be finite. In the computational model for SIFTS the pixels in the array will be of finite width and number. However, a Fourier transform calculation always assumes infinite bounds. Therefore, modifications have to be made to the computations so as to emulate infinite data sets.[2]

The need for foot removal comes when we look at what the Fourier transform is doing with discrete data. Since it assumes infinite data, the finite data created computationally (or collected experimentally) must be multiplied by some *boxcar* function that is one throughout the defined domain and zero everywhere else. Because it is

true that

$$f_{\text{boxcar}}(x) \supset \sin\left(\frac{2\pi\sigma}{\sigma}\right)$$

and by definition

$$f(x) \supset F(\sigma)$$

we have as a result

$$f(x) \star f_{\text{boxcar}}(x) \supset F(\sigma)\sin\left(\frac{2\pi\sigma}{\sigma}\right)$$

When a DFT is used to retrieve a spectrogram, such as $F(\sigma)$, it will be distorted by a sinc function. The sinc function has lobes on both sides of a central peak. These lobes will create symmetric *feet* or ringing effects on peaks in $F(\sigma)$ that represent false sources of spectral energy at nearby wavenumbers.

In order to combat this unrealistic computational effect, the data is multiplied by some apodizing, or window, function that does not have such abrupt changes as a boxcar function.[2] Given a symmetric interferogram, these functions will be of a rounded nature such as a gaussian curve or a half-period cosine wave that will be one at zero OPD and will slowly taper the ends of the interferogram by reaching zero at the extremes of the domain. The combined effect is a weighting of data near the origin against data at the extremes of the domain.

Many such window functions exist and each is used when deemed appropriate for its situation. Under optimal conditions, the apodizing function will minimize the deleterious effects of finite data. However, the cost is widened peaks and, therefore, lower resolution.

3.4 Maximum Resolutions

The relationship between resolution and sampling determines the maximum resolution available for the simulated interferogram $f(x)$ given the number or data points N in the input spectrogram. It also determines the maximum resolution that can be acheived in the retrieved spectrum $F'(\sigma')$ given the number of detector elements in the array.

If more samples are taken (or more detectors of fixed width are used), the result is a longer interferogram with greater $x_{\max}$. Intuitively, it should be clear that the longer an interferogram is, the greater the available frequency resolution. For overlaping waves, smaller differences in frequency will take longer to show up. It turns out that the exact relationship is given by[2]

$$\Delta\sigma = \frac{1}{x_{\max}} \tag{5}$$

The same type of relationship exists when going the other direction. The largest frequency in the spectrogram determines the spatial resolution of the interferogram:

$$\Delta x = \frac{1}{\sigma_{\max}} \tag{6}$$

The problem of aliasing further limits the maximum theoretical resolution. The Nyquist criterion states that for every N data elements, only $\frac{N}{2}$ distinct frequencies can be derived before aliasing provides false characteristics.[3] For SIFTS, this has direct implications on the ability to achieve high resolution spectral retrievals since the number of data elements will be limited by the number of detectors present in the sensor system.

Because the wavenumber σ is a spatial frequency, $1/\sigma_{\max}$ is the smallest spatial period. To meet the Nyquist criterion, we must take at least two samples every spatial period. Thus,

$$2\Delta x \leq \frac{1}{\sigma_{\max}} \tag{7}$$

Since

$$\Delta x = x_{\max}$$

we have

$$\frac{x_{\max}}{N} \leq \frac{1}{2\ \sigma_{\max}}$$

Substituting in Eq. (5) and rearranging, the relation becomes:

$$\sigma_{\max} \leq \frac{\Delta\sigma N}{2} \tag{8}$$

Or in terms of the interferogram:

$$x_{\max} \leq \frac{\Delta x N}{2} \tag{9}$$

These relations giving the maximum possible resolutions are valid for both the calculation of the simulated interferogram and fo the calulation of the retrieved spectrum. For any calculation after the model simulates the the effects of the detector array, the primed notation is used.

4 Computational Model Code

4.1 Formulating Spectra and Interferograms

The forward model will test the effects of the SIFTS sensor by first establishing an "Original Spectrum". Such a spectrum, as shown in the top left of Fig. 1, could be a collection of experimental atmospheric data or a case study spectrum created for our purposes. Because the original spectrum is only a discrete version of a real-world, continuous spectrum, both $\Delta\sigma$ and $\sigma_{\max}$ must have better resolution and greater range than the SIFTS system would be able to attain. Usually $\Delta\sigma = 0.1$ cm^{-1} and $\sigma_{\max} = 120,000$ cm^{-1}. These choices determine, respectively, the best possible interferometric range and resolution. They are chosen in order to minimize the effects of using discrete data to model infinite, continuous realistic spectral characteristics[2].

The second step in creating the spectra and interferograms was necessitated by the notation and usage of data by the Fast Fourier Transform (FFT) algorithm. Since a computer cannot store data in an array with negative indicies (corresponding to negative frequencies in a complex Fourier transform), a special organizational scheme was created to go along with the use of the FFT. This scheme allowed for negative frequencies to be stored in an array after the positive.

For example, if a spectrum has N data points indexed from $n = 1$ to N, in order to store the N points as distinct individual frequency contributions, the negative frequencies ($-\sigma_{\max} < -\sigma_n < -\sigma_{\min}$) are stored from $N/2 \leq n \leq N$ and the positives ($0 < \sigma_n < \sigma_{\max}$) stored from $1 \leq n \leq N/2$ where the $N/2$ corresponds to both $\sigma = \sigma_{\max}$ and $\sigma = -\sigma_{\max}$. This notation both implies that N data points will only describe $N/2 + 1$ distinct frequencies and, for our case, N' detectors will limit our spectral range and resolution by only describing this same amount of wavenumbers.[6]

In order to work with this, all spectra are created such that the whole wavenumber range was specified and then copied backwards in the manner just described resulting in a spectrum twice as large. Consequently, after the IDFT is taken of the spectrum, the interferograms which hold the same form of negative OPDs after the positive are composed of N or N' data points.

4.2 Other DFT Considerations

In addition to these above restrictions, the nature of the interference phenomenon demanded that the interferogram be both real and even mathematically. The interferogram has no complex component and $f(-x) = f(x)$. This relation for Fourier transform spectrometers has been previously derived.[5] The model works when the Fourier transform of a real and even function is real and even.[4]

Single-sided interferograms were also assumed for the forward model. This implies that only one side of the interferogram is placed on the detector array such that one half of the symmetric interference occupies the whole the array. It is common practice in Fourier transform spectroscopy for single-sided interferograms to be used based on the mathematically even nature of the interferogram.

This technique allows for utilizing the entire detector array and in doing so achieves a value of $x_{\max}$ twice as large, thereby doubling the resolution. Also, it eliminates redundant use of detector elemets. This approach also doubled the interferometric resolution and doubled the retrieved spectral range. However, determining the exact center (zero OPD) is very often nearly impossible to find experimentally and will therefore cause baseline phase errors in the FFT calculation and skew results. For this reason, double-sided configurations are also commonly used when sensor resolution is significantly be-

[2]See Section 5.3.2 for a full explanation.

yond the requirements.

Since the interferograms made from the input spectra used in the forward model are discrete data and not a continuous light source, the model knows exactly where the zero OPD point is and will not produce phase errors.

4.3 Pixelization/Detector-Averaging

The pixelization effects of the detector array are the most basic of the represented quantities in the detection phase. Since the interferogram would always be real, even, symmetric and always contain an even number of data points, certain restrictions were placed on the averaging procedure.

The use of discrete data to simulate both reality and the response of the SIFTS sensor causes a number of difficulties. The simulated radiation landing on the detector array consists of discrete points. However, there is no capability in the model for averaging half of a point or possibly sharing points between detectors. Also, the resolution and range choices made for the original spectrum dictate the detector choice procedure. The organizational scheme needed by the FFT allows only for even amounts of detectors with the same number of points averaged with each detector. Although this is a minor detail, it did limit the possible numbers of detectors that could be simulated.

The digitally simulated interferogram $f(x)$ is the IDFT of the original spectrum $F(\sigma)$ and it is averaged in order to display the effects of pixelization. From here, the point at which the maximum OPD is found and all other data beyond this point is thrown out because of Eq. (5). Then, all whole number common factors are found based on this number and all possible choices of even number of detectors and how many points will be averaged per detector are given for the user to decide. The quantity of points per detector was denoted as p. Obviously, the choice of the number of detectors will effect how many points are averaged together. More detectors will mean less points per detector and smaller value for $\Delta x'$, which increases the retrieved spectral range. Unfortunately, because of Eq. (6), more detectors does not necessarily increase resolution.

The actual algorithm for averaging points in the pixelization process is very simple. The approach taken is to average the interferogram's data set p points at a time from beginning to end. The restrictions discussed earlier allow this to work since the only choices for detector configuration would make each detector get p points exactly and the data would be again symmetric, real and even. Several other averaging schemes were attempted, but resulted in unknown computational effects and unexplainable results. This scheme produces a data set that was immediately ready for the DFT and transformation back into the spectrogram, $F'(\sigma')$.

4.4 Fill-Factor

Preliminary studies were done with fill-factor, but were abandoned due to time constraints.

4.5 Non-Uniformity of the Detector Array

The effect of non-uniformity of the detector array was included in some versions of the forward model. However, for reasonable non-uniformities, its effect was minimal compared to those of the pixelization process. Therefore, the results are not reported here.

The simulation of non-uniformity in the detector array was achieved by multiplying each detector value by a random number. This number was determined by using a normal distribution with the mean, $\mu = 1.0$ and standard deviation, $\sigma = 0.1$.

4.6 Background/Photon Noise

Up to this point, no code has yet been written or implemented in the model for showing the effects of background or photon noise on the resolution and range of the SIFTS sensor.

4.7 Mathematical Processing

In the retrieval phase of the model, apodization is an important step when testing spectra

with considerable absorption regions and abrupt changes.

Apodization is done immediately preceeding the DFT of the pixelized interferogram. Since the data set is situated such that the maximum OPD was in the center, the array of data was doctored in order that the zero OPD was in the center so that the apodizing function would line up correctly. Prior to the DFT, the new apodized version of $f'(x')$ was placed back in its original configuration.

The apodization function is chosen such that feet and other spikes are minimized. Currently, a blackman window is being used. However, a careful investigation should be done to determine if this is the best window function.

4.8 Retrieved Spectrum Output

After the retrieved spectrum has been obtained, $F'(\sigma')$ can be compared with input spectrum $F(\sigma)$. The resolution of the retrieved spectrum is usually significantly less than the original, so some care must be taken to plot both spectra on the same scale.

5 Results

5.1 Input Spectra

In testing the forward model, case study spectra are chosen to determine the results of the pixelization process. Of great importance is the ability to decipher the effects that pixelization has on certain spectral features such as absorption regions and spectra closely related to those that SIFTS would be analyzing in space applications. For this reason, our test cases consist mainly of simple blackbody spectra at atmospheric temperatures and similar blackbody spectra with artificial absorption regions.

Future investigations with the forward model should utilize the results of previous experiments by taking actual high resolution atmospheric data and using it as an input spectrum. Figure 2 shows a sample spectrogram provided by NASA/Langley. Unfortunately, the spectrogram was not in a format from which the data could

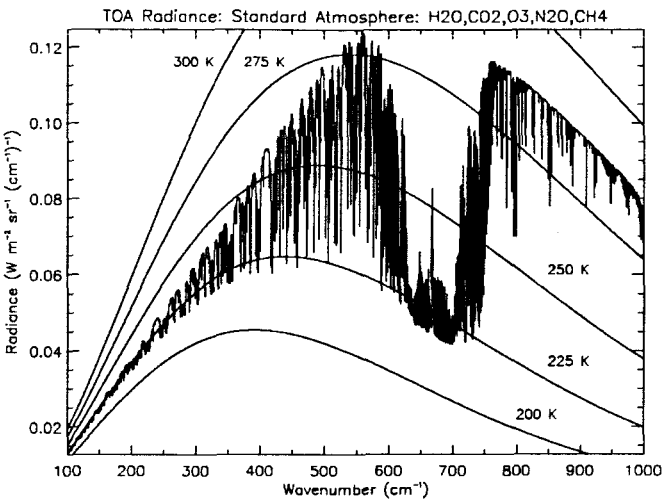

Figure 2: Example of Spectrogram of Far-IR region determined experimentally.

readily be extracted. Therefore, this spectrogram was not used as an input to our computational model. The background lines in Fig. 2 show blackbody radiation spectra at different temperatures. Based on a comparison between the actual specta and the blackbody spectra, we chose to use blackbody radiation at $T = 275$ K as the standard test input to our computational model.

5.2 Resolution and Range Tradeoffs

The relationships derived in Section 3.4 indicate that the tradeoffs involved with the SIFTS sensor will be resolution and range. For example, because of Eq. (8), N' detectors capable of $\Delta\sigma'$ resolution will produce a maximum range of $\sigma'_{\max}$. However, doubling the resolution to $\Delta\sigma'/2$ cuts the maximum range in half.

It is instructive to use numbers that reflect the realistic values presented in Fig. 2. For a $\sigma'_{\max} = 1,000\,\mathrm{cm}^{-1}$ with 500 detectors, our spectral resolution at its best can only be $\Delta\sigma' = 4$ cm^{-1} according to Eq. (8). If there 1,000 detectors, then it is possible to obtain $\Delta\sigma' = 2$ cm^{-1}. Fortunately, if a single-sided interferogram is used (as is assumed in our computational model), there is effectively twice as much data which will double the resolution.

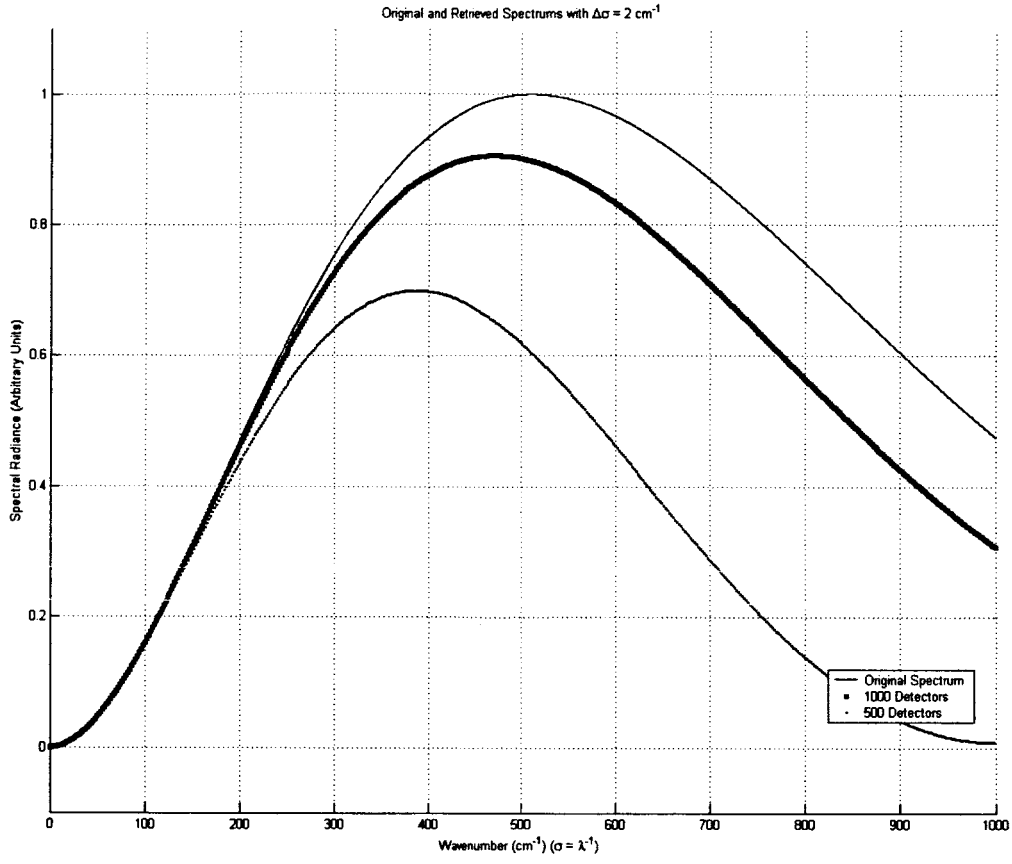

Figure 3: Retrieved spectra from the model with $\Delta\sigma' = 2$ cm^{-1}. (Note: all figures produced by the computational model consist of discrete data. Graphical extrapolation and/or nearness of data points makes the graphs appear to be continuous.)

5.3 High Wavenumber Attenuation

So far, the computational model's most significant achievement is the prediction of attenuation at high wavenumbers caused by the sampling and averaging of interferometric data by each detector. When any interference pattern is sampled, the effects of averaging will smooth out the highest frequencies first. Thus, the retrieved spectrum will have attenuated higher frequencies.

5.3.1 Blackbody Radiation Spectra

Figure 3 shows the original blackbody and subsequent retrieved spectrum output by the model with $\Delta\sigma' = 2$ cm^{-1}. The averaging effect is clearly seen as the intensity of the spectrum at the higher wavenumbers are significantly more attenuated than that at the smaller σ. Notice also that the figure shows retrievals done with both 500 and 1,000 detectors and that the lesser number of pixels causes significantly more attentuation. This is easily explained by realizing that if fewer detectors are present, each pixel must average over a greater width (remember that we are assuming the interferogram can always be adjusted to cover the entire detector array). If the detector width $\Delta x'$ is larger, the retrievable spectral range is decreased. In addition, if a pixel averages over a greater area, there is less sensitivity to higher frequencies.

As the spectral resolution requirement is increased for a retrieved spectrum, attenuation will

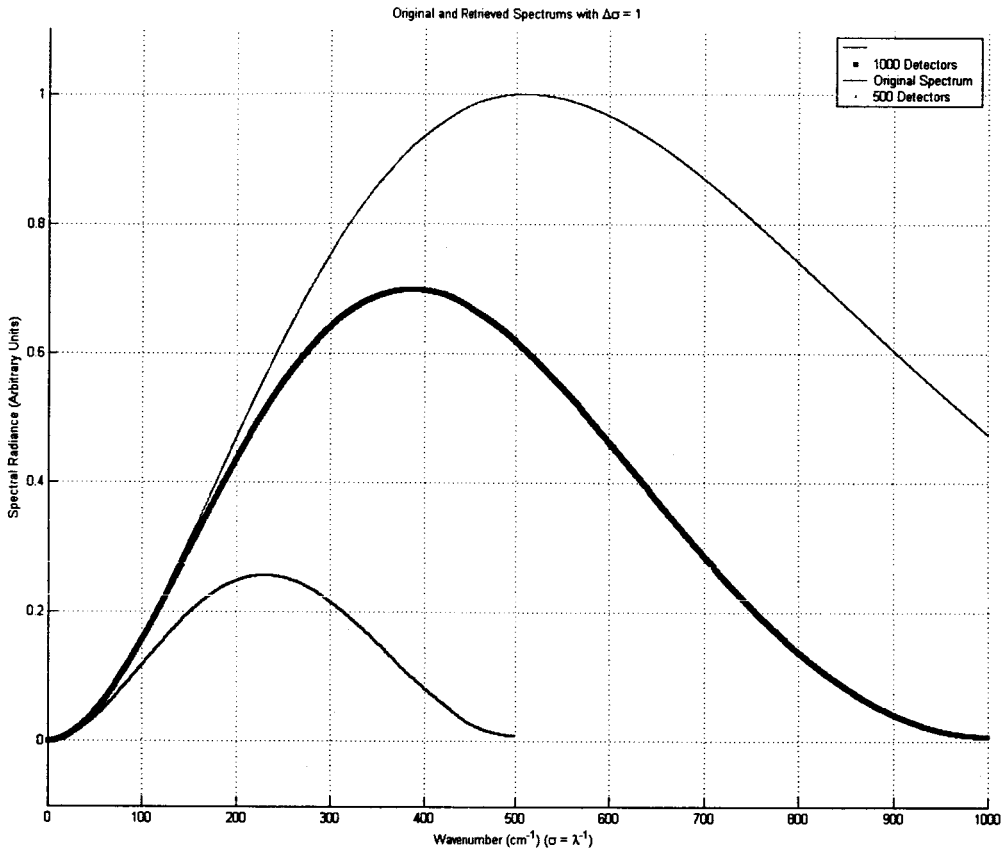

Figure 4: Retrieved spectra from the model with $\Delta\sigma' = 1$ cm^{-1}.

become an even larger problem for the SIFTS sensor. For instance, Fig. 4 shows the results when $\Delta\sigma' = 1$ cm^{-1}. The 500 and 1,000 detector retrieved spectra have attenuated much more than those in Fig. 3. This is due to the increased resolution requirement which has lengthened $x_{\max}$ and therefore forced each pixel to average over an even larger area producing greater attenuation at high wavenumber. Note also that at this resolution, it is impossible for the 500 detector array to yeild data beyond 500 cm^{-}1.

The model predicts that the opposite will result if lower resolution is required. A test with $\Delta\sigma' = 4$ cm^{-1} not only doubles the non-aliasing range ($\sigma_{\max}$) but decreases the active averaging area of each pixel. Figure 5 shows these results. Resolution can be sacrificed for greater range and less attenuation at higher wavenumbers.

5.3.2 Spectral Radiance Attenuation Plots

The percentage of spectral radiance *lost* due to the pixelization process is displayed in Fig. 6 for the retrievals in Figs. 3, 4 and 5. Here, $\Delta\sigma' = 1, 2$ and 4 cm^{-1} for both 500 and 1,000 detectors. Figure 6 is a vivid illustration of how the attenuation increases with wavenumber. In addition, it shows how this effect increases dramatically with greater resolution requirements.

Notice that although six attenuation profiles are graphed in Fig. 6, only four our visible. This is the result of the predictions made earlier with the Nyquist criterion that N' detectors with $\Delta\sigma'$ resolution will produce the same results as $N'/2$ detectors at $2\Delta\sigma'$ resolution.

The spectral radiance attenuation plots aid in

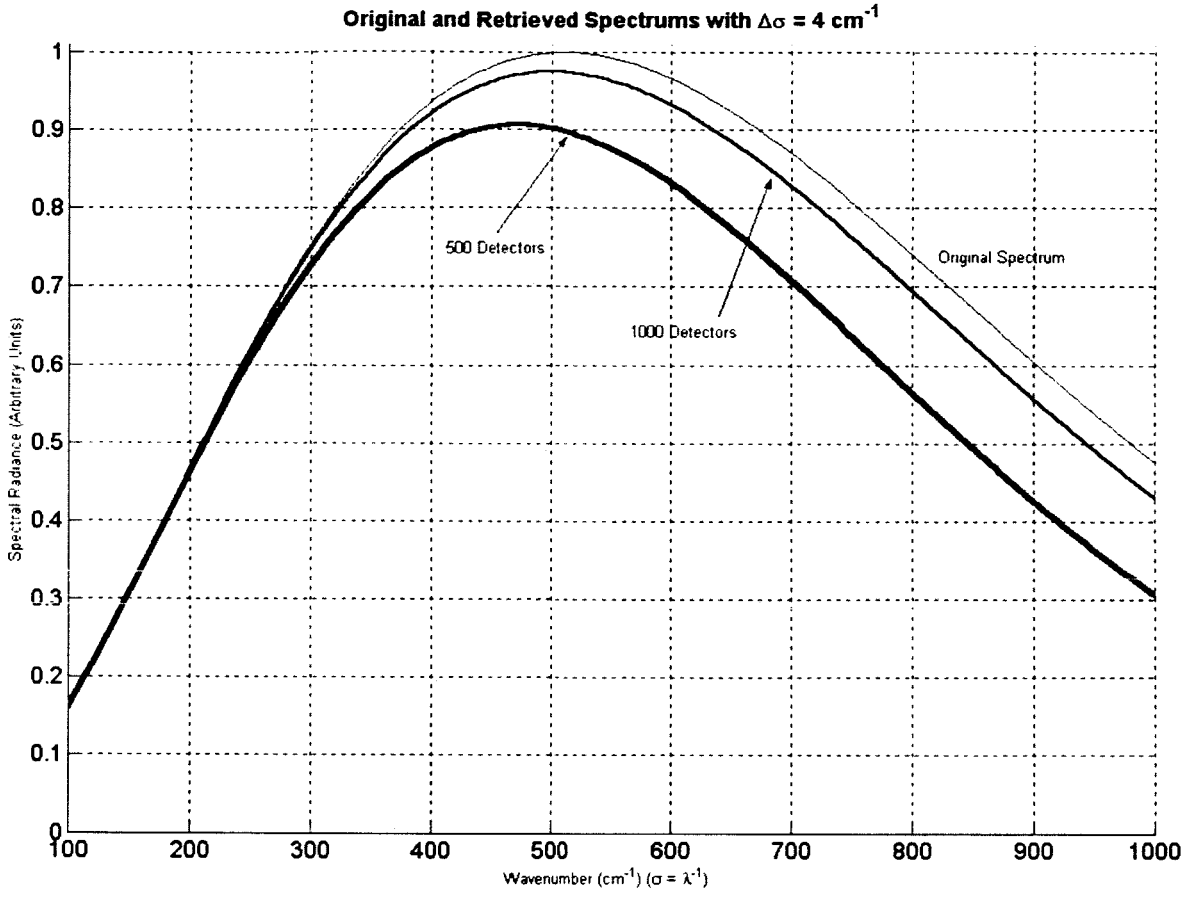

Figure 5: Retrieved spectra of 500 and 1,000 detectors with $\Delta\sigma = 4$ cm^{-1}. By trading lower resolution the range has been increased and the attenuation minimized.

testing the computational model. If the original spectrums were created with $\sigma_{\max}$ chosen as some arbitrary number higher than $\sigma'_{\max}$, then the choice of $\sigma_{\max}$ strongly affects the results that the model predicts because of the dependence of Δx on $\sigma_{\max}$. If Δx is of similar width compared to the detector width, p will be smaller and the effects of averaging will not be as harsh as if Δx was much smaller than the width of each detector.

Figure 7 shows the effects of increasing $\sigma_{\max}$ (decreasing Δx) on the attenuation of retrieved spectrums with 500 and 1,000 detectors. Notice that the effects of increasing the maximum spectral range seemed to saturate around $\sigma_{\max} = 120,000$ cm^{-1}. It was found that no significant additional attenuation occurred beyond this point. Therefore, as indicated in Sec. 4.1), this was the maximum value used in all model calculations.

5.3.3 Blackbody Spectra with Absorption

Spectra with sharp, artificial regions of absorption were also tested with the model to determine the effects of the SIFTS system on smaller spectral features.

Figure 8 shows a retrieved spectrum with $\Delta\sigma' = 2$ cm^{-1} and 1000 detectors. On this same graph, the spectral percentage attenuation is plotted because it highlights the effects that detector averaging has on the absorbed regions. A rounding off at the edges of the absorption

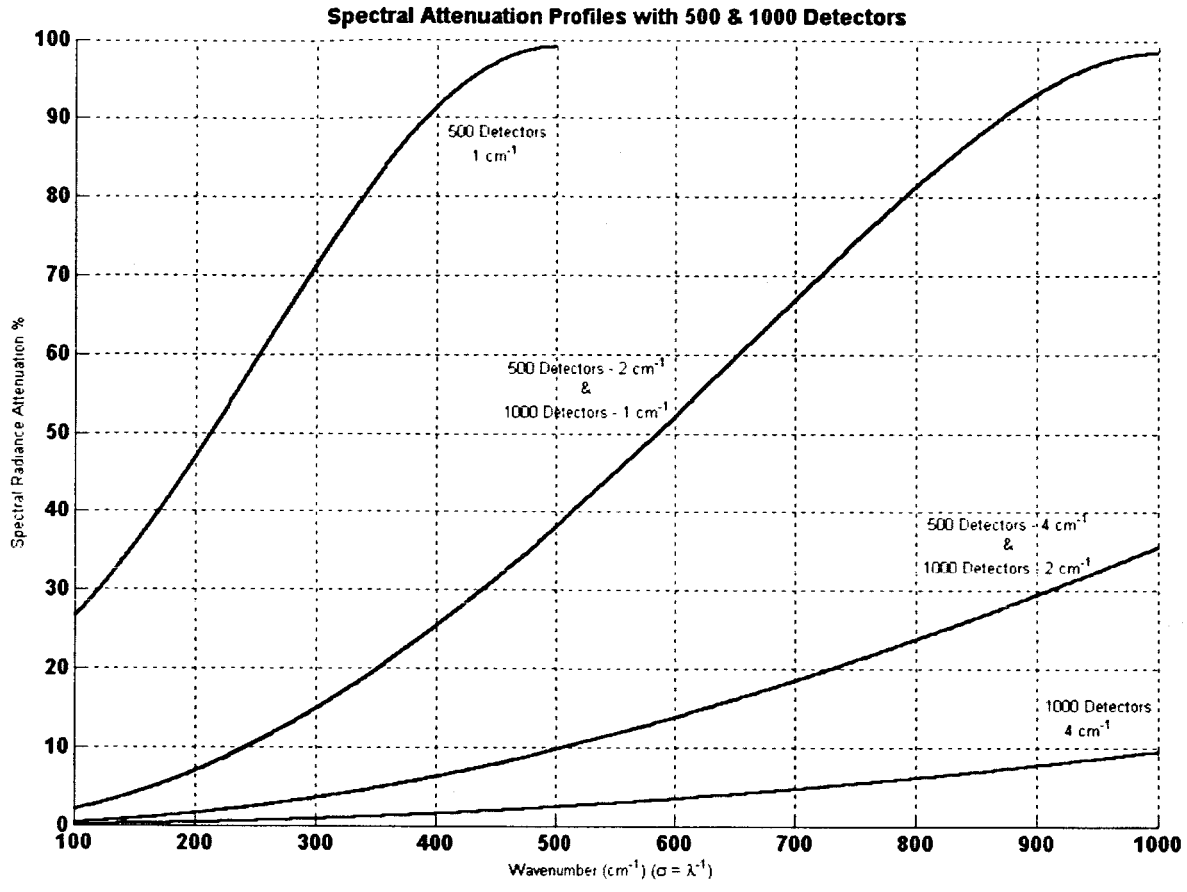

Figure 6: Spectral percentage attenuation plot for 500 and 1,000 detectors at three different spectral resolutions. The cases of $\Delta\sigma' = 2$ cm^{-1} with 500 detectors and $\Delta\sigma' = 1$ cm^{-1} with 1000 detectors are the same as predicted by Nyquist. Similar results occur with $\Delta\sigma' = 4$ cm^{-1} with 500 detectors and $\Delta\sigma' = 2$ cm^{-1} with 1000 detectors.

regions creates large errors in spectral radiance.

Note also the absorbed regions, especially around 275 cm^{-1} in Fig. 8, attenuate in similar amounts to the unabsorbed regions surrounding them. This suggests that the high wavenumber attenuation depends on the arrangement of detectors and not on the amount of spectral radiance in any one region.

The addition of absorption lines into case study spectra also shows the necessity for mathematical processing such as apodization in the model. Figure 9 shows a retrieved spectrum and its corresponding apodized calculation. The effect of a window function on regions where abrupt changes occur, such as in absorption lines, appears to average out false oscillations.

6 Summary and Conclusions

The computational model that has been developed for the simulation of the SIFTS sensor provides an important method for studying the feasibility of SIFTS for far-IR spectroscopy and its possible presence among atmospheric sensors in orbit. The relationships developed and modeling presented should frame the issues, particularly those related to spectral resolution and range.

The results shown by the model suggest an important and possibly detrimental characteristic of the detector array's effects on retrieved spec-

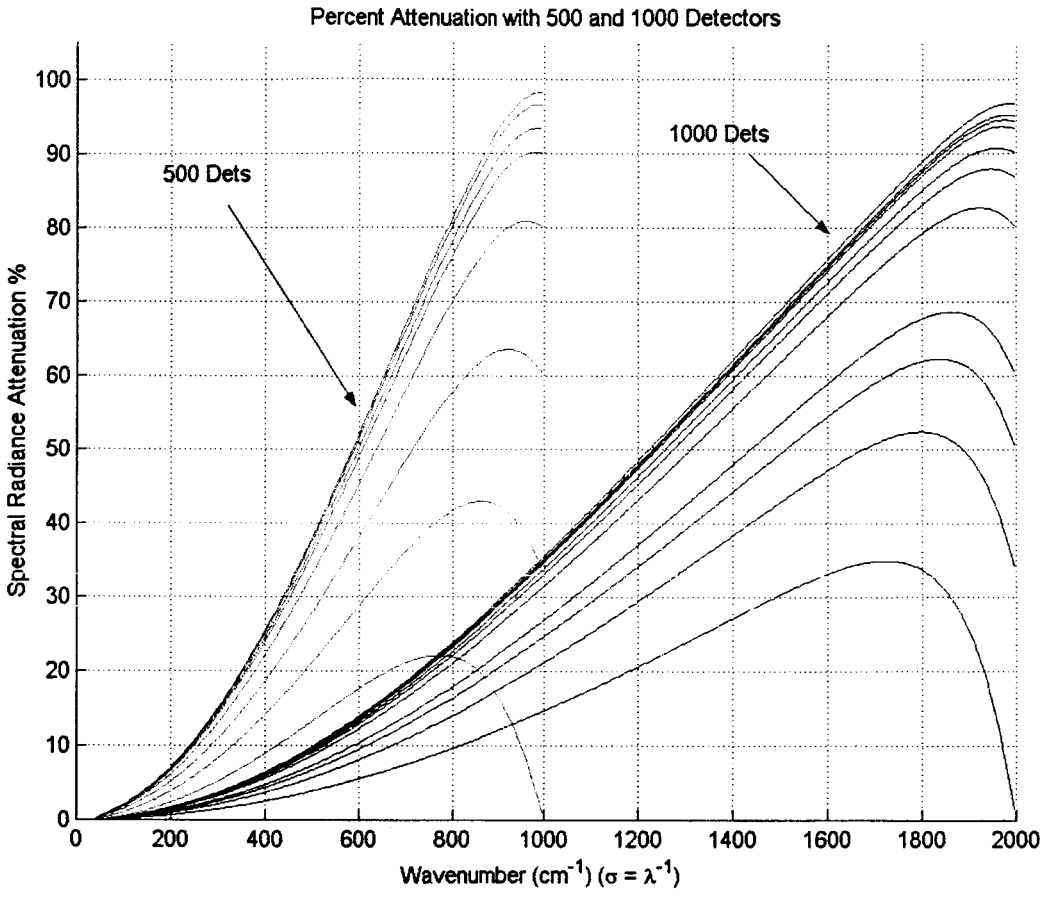

Figure 7: Graph showing results of changing $\sigma_{\max}$ from 2,000 to 120,000 cm^{-1}.

tra. Since far-IR spectroscopy is heavily concerned with relative abundances of spectral energy in certain absorbed regions, the dependence of attenuation on wavenumber may be a difficult obstacle to overcome.

However, the spectral attenuation plots introduced here provide a possible solution. Each attenuation plot provides a unique signature of the attenuation of a certain detector configuration. It should be possible, if these signatures are verified experimentally, to use these results to compensate for the system induced high wave number attenuation.

The computational model developed in this work is not yet complete. The effects of fill-factor and photon noise have not been incorporated. An attempt has been made to model detector array non-uniformity, but the preliminary results indicated that this should not be a significant factor. Although more work should be done, so far it appears that the attenuation effects resulting from detector averaging are very likely to be the primary performance limitation.

Perhaps the continuing advances in infrared detector array technology will improve the inherent performance limitations of the SIFTS system. Certainly, more detectors will increase the unaliased range of far-IR calculations and decrease the spectral attenuation in regions of interest.

References

1. Mlynczak, Dr. Martin, *Frontiers in Passive Atmospheric Remote Sensing,* Creativity and Innovations Proposal to NASA/Langley

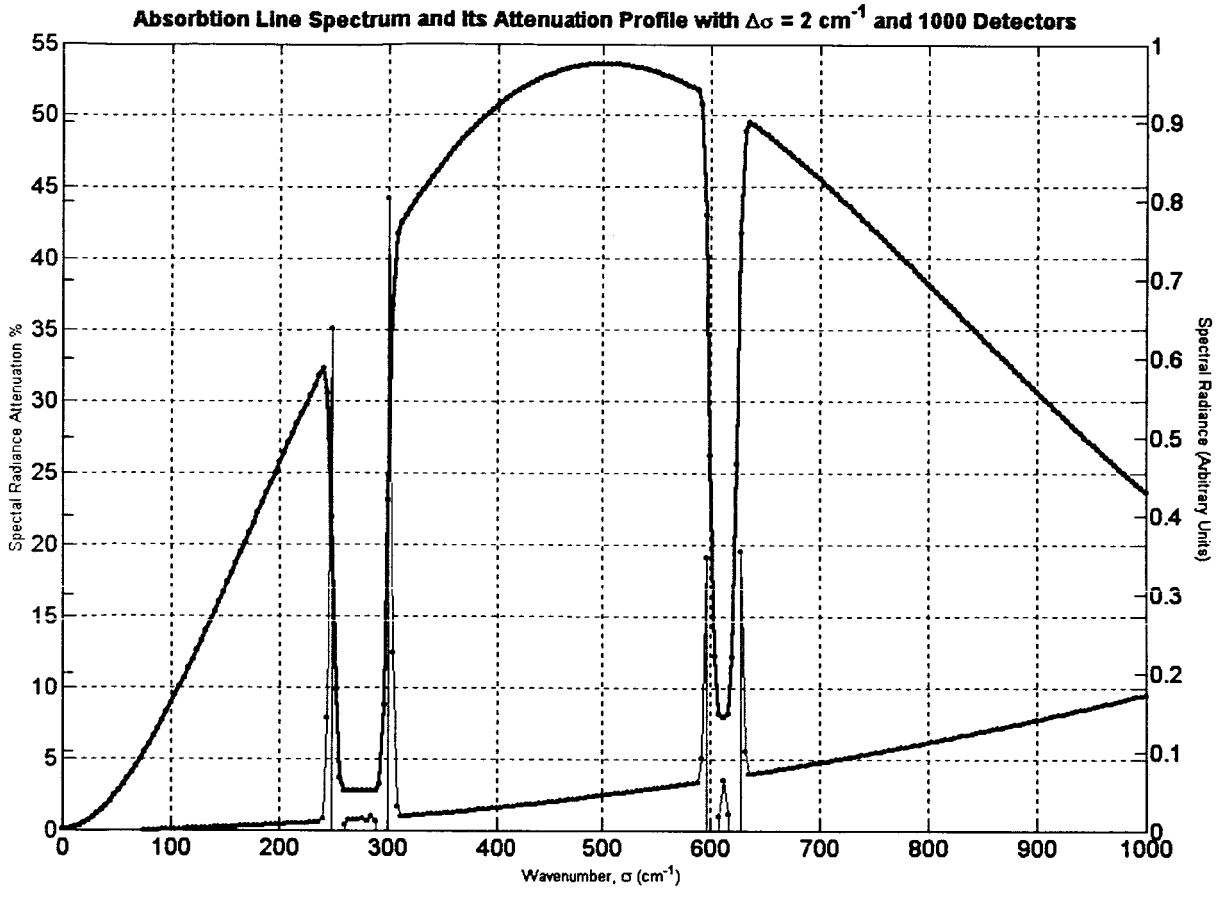

Figure 8: Graph of retrieved spectrum ($\Delta\sigma' = 2\ \mathrm{cm}^{-1}$ and 1,000 detectors) with two artificial absorption regions. Note: spectral radiance scale on right and attenuation percentage on left.

Research Center, 2000. Hampton, VA.

2. Bell, Robert J., *Introductory Fourier Transform Spectroscopy.* Orlando: Academic Press, Inc., 1972.

3. Williams, Ron, *Spectroscopy and the Fourier Transform.* New York: VHC Publishers, Inc., 1996.

4. Bracewell, Ronald, *The Fourier Transform and Its Applications.* New York: McGraw Hill, 1986.

5. Pedrotti, Frank L. and Leno S. Pedrotti, *Introduction to Optics.* New Jersey: Prentice Hall, 1993.

6. Weisstein, Eric, "Discrete Fourier Transform," *Eric Weisstein's World of Mathematics.* Wolfram Research: CRC Press LLC., 1999. <http://mathworld.wolfram.com/DiscreteFourierTransform.html>.

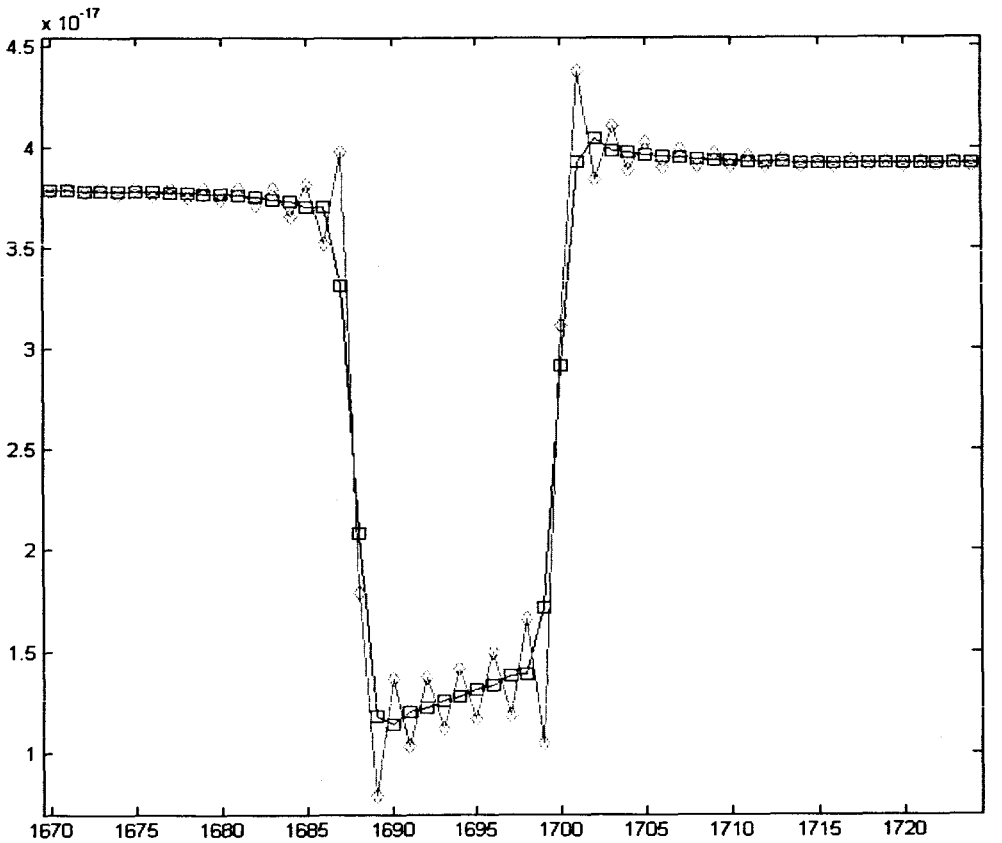

Figure 9: Close-up view of an absorption region in a retrieved spectrum created by the model. The apodization process dampens the ringing often associated with sudden changes in discrete Fourier transform calculations.